

How cold was the Last Glacial Maximum?

Thomas Schneider von Deimling, ¹ Andrey Ganopolski, ¹ Hermann Held, ¹ and Stefan Rahmstorf ¹

Received 3 April 2006; revised 30 May 2006; accepted 7 June 2006; published 27 July 2006.

[1] We present a new approach to estimate the magnitude of global-mean cooling (dT_{LGM}) at the Last Glacial Maximum (LGM) relative to the pre-industrial climate, by combining an ensemble of coupled climate model simulations with empirical constraints on regional cooling inferred from proxy data. We have generated a large ensemble of paired runs (\sim 100) for pre-industrial and LGM boundary conditions with different versions of the same climate model of intermediate complexity. The model ensemble covers a broad range of climate sensitivities and produces a similarly broad range of dT_{LGM} (4.3–9.8°C). Using reconstructed tropical SST cooling, we constrain the range of dT_{LGM} to 5.8 ± 1.4 °C, which is corroborated by proxy data from other regions. This cooling is considerably larger than most estimates of previous LGM simulations. The reason is that most models did not account for the effect of atmospheric dust content and vegetation changes, which yield an additional 1.0-1.7°C global cooling. Citation: Schneider von Deimling, T., A. Ganopolski, H. Held, and S. Rahmstorf (2006), How cold was the Last Glacial Maximum?, Geophys. Res. Lett., 33, L14709, doi:10.1029/2006GL026484.

1. Introduction

[2] The time period around 21 kyr before present, commonly referred to as the Last Glacial Maximum (LGM), is characterized by the maximum volume of northern hemisphere ice sheets, along with a pronounced cooling over most of the globe. This cooling is manifested in global mean temperature, which is arguably the most important characteristic of a particular climate state, reflecting the overall planetary energy balance. Knowledge of global mean cooling during the LGM will allow us to put the magnitude of future climatic changes into context. Global mean cooling is also crucial to infer *climate sensitivity*, which is defined as the global mean temperature change per unit of radiative forcing change (or, more specifically, the global temperature change dT_{2x} for CO_2 doubling from its pre-industrial value). Thus an accurate estimate of dT_{LGM} is of crucial importance when determining the sensitivity of Earth's climate system to changes in the radiation budget, based on past climate changes. Inferences of climate sensitivity from glacial climate data [e.g., Lorius et al., 1990] have been hampered by having to make assumptions about the ratio of local (e.g., in Antarctica) to global temperature changes.

[3] Global mean cooling during the LGM is difficult to determine accurately. Proxy data (e.g., ice or sediment cores) are generally local by nature and too sparse to

combine by spatial averaging into a meaningful global mean. Model based estimates readily give a global mean value, but different model estimates range from 2°C to 10°C, even though most modeling results fall into a more narrow range (3–6°C [Masson-Delmotte et al., 2006]). These large uncertainties are due to uncertainty both in the forcing (many models even use only a subset of the relevant forcings) and in the models themselves (the climate sensitivity is still considered to be uncertain by a factor of three, see the 1.5–4.5°C range given by Intergovernmental Panel on Climate Change [2001]).

- [4] A better approach therefore is to combine proxy data with a large model ensemble. The effect of uncertainty in forcing or model is then greatly reduced by constraining the model results with proxy data, rejecting all global mean cooling values inconsistent with the data. The model ensemble, on the other hand, provides a physically consistent way to derive a global mean value from the local information provided by proxy data, that is, consistent with what we know about the forcing and about plausible climate physics, as mapped out by the model ensemble. This is the approach taken in our study.
- [5] We first generate a large ensemble of model versions with different parameter choices, resulting in different feedback strengths and hence climate sensitivities, thereby accounting for uncertainty in the model response. We run this ensemble for a complete set of main glacial boundary conditions (see next section), including dust and vegetation changes. We then use proxy data from specific regions to constrain the ensemble, in particular to estimate what range of simulated global LGM cooling is consistent with reconstructed regional temperature change.

2. Experimental Design

- [6] We use a climate model of intermediate complexity (CLIMBER-2), consisting of a dynamical-statistical 2.5-dimensional atmosphere model, coupled without flux adjustments to a multi-basin, zonally averaged ocean model [Ganopolski et al., 1998; Petoukhov et al., 2000]. The model includes parameterization of sea ice transport and iceberg calving from the ice sheets, assuming the latter to be in equilibrium with climate forcing.
- [7] Simulating the LGM climate crucially depends on i) the radiative forcing of the climate system resulting from the pronounced difference between modern and glacial boundary conditions, and on ii) the model sensitivity governing the amplification and damping of this forcing by the model-inherent feedbacks. We have applied PMIP-2 boundary conditions for greenhouse gas concentrations (an equivalent CO₂ concentration of 167 ppm), ice sheets and land distribution/elevation and orbital parameters. For all ice-free grid cells we use the same river run-off routing

Copyright 2006 by the American Geophysical Union. 0094-8276/06/2006GL026484\$05.00

L14709 1 of 5

¹Potsdam Institute for Climate Impact Research, Potsdam, Germany.

scheme as for present day conditions. Additionally we account for forcing contributions resulting from changes in atmospheric dust content and vegetation. Especially for the tropics, dust may have exerted a radiative cooling of similar magnitude as CO₂ forcing [Harrison et al., 2001; Claquin et al., 2003]. As our climate model does not include a dust cycle, radiative effects of dust are prescribed as spatial patterns of monthly top-of-the-atmosphere anomalies of the short-wave radiation, which have been inferred from several ECHAM-5 simulations [Stier et al., 2004; M. Werner, personal communication, 2004]. Vegetation cover is prescribed from a LGM simulation with the standard version of CLIMBER-2 with an interactive vegetation scheme. Thereby, vegetation changes are treated in this study as an additional forcing rather than as a feedback.

[8] We have set up an ensemble of model versions (with differing climate sensitivities) by perturbing 11 model parameters, which mainly affect our model's feedback strengths (water vapor, lapse rate, cloud, and albedo). We sampled this parameter space by applying an efficient Monte-Carlo method and run the ensemble of 1,000 model versions for pre-industrial and 2xCO₂ boundary conditions. The resulting range of climate sensitivity ranges from 1.5-5.5°C. We then constrain this ensemble to a set of model versions (123 model members), which all are consistent with global mean characteristics of present-day climate [Schneider von Deimling et al., 2006] and run those model versions for all glacial boundary conditions. We infer the range of global LGM cooling by calculating the difference in simulated global mean surface temperature between the LGM and pre-industrial climate.

[9] In order to specify the contribution of the individual forcings to total LGM cooling we performed a factor analysis similar to that of Ganopolski [2003]. To separate the magnitude of CO₂ induced cooling from dT_{LGM}, we additionally performed an ensemble of simulations, for which we applied pre-industrial boundary conditions, but prescribe the CO₂ concentration to its glacial value of 167 ppm (also accounting for glacial changes in CH₄ and N₂O which are not included in CLIMBER-2 radiative scheme). The difference in the simulated temperature between this "CO₂ only" experiment and the pre-industrial runs yields that fraction of the glacial cooling which is caused by CO₂ concentration changes. We further generated three additional ensembles by successively adding the glacial forcings of ice sheets, vegetation cover and dust and determine the impact of individual forcings by taking the difference between 2 successive ensembles. It should be noted that this methodology does not account for nonlinearities in the system response. If we calculated the CO₂ affected cooling as the difference between the total LGM cooling and an ensemble of simulations where all boundary conditions are set to glacial, but CO₂ fixed to its pre-industrial value of 280 ppm, we infer a slightly larger fraction of CO₂ induced cooling.

3. Paleo Data Constraints for Global LGM Cooling

[10] Global coverage of paleo records is too sparse to reconstruct global LGM cooling with satisfactory accuracy. Yet for specific regions an estimate of large-scale regional

temperature change can be inferred from proxies and then be applied to constrain the simulated regional LGM climate.

[11] Numerous data from sediment-cores are available from tropical ocean sites. To constrain our ensemble we use an objectively interpolated data set [Schäfer-Neth and Paul, 2003], which comprises a large set of sediment-cores of stringent quality and age control. We focus on the tropical Atlantic (20°N-20°S), as this region is densely covered by proxy sites and thus offers the chance to estimate a representative spatial mean cooling. Those data are based on GLAMAP reconstructions [Sarnthein et al., 2003], having been derived from transfer functions of faunal assemblages of foraminifera. Accounting for reconstruction uncertainties of each data core and for uncertainty in the pattern of sea surface temperature (SST) cooling, this data set yields a range of spatially averaged tropical Atlantic SST cooling of $3.0^{\circ} \pm 0.9^{\circ}$ C (2σ , see Appendix in work by Schneider von Deimling et al. [2006]).

[12] In addition we also consider other data types and regions. Tropical land data are cautiously discussed as the data coverage is sparse and temperature reconstruction complicated by uncertainties in potential lapse rate changes. Concerning high latitudes, ice cores provide a valuable archive, but only for a limited number of sites in Greenland and Antarctica. Given the large spatial extent of the tropical oceans and the progress of SST reconstruction techniques made in recent years, we focus on this region as primary constraint of our model ensemble. We will show in section 5 that proxies from tropical land sites, Antarctica and Greenland constrain our ensemble very consistently.

4. Model Results

4.1. Global LGM Cooling

[13] Our ensemble simulations allow us to estimate the range of global LGM cooling from a set of model versions with differing feedback strengths and climate sensitivities. Unconstrained by data, our ensemble simulates a decrease in global mean surface air temperature (SAT) of 4.3-9.8°C between pre-industrial and glacial climate. The glacial cooling in different regions is tightly linked to global LGM cooling [Schneider von Deimling et al., 2006] and thus can be used to constrain dT_{LGM}. Next, we derive a subset of ensemble members whose regional temperature response (i.e., the simulated tropical Atlantic SST cooling) falls inside the discussed proxy data range $(3.0^{\circ} \pm 0.9^{\circ})$. This subset has 64 members with LGM global cooling in the range 5.8 ± 1.4 °C. This inferred cooling is substantially larger than in recent PMIP-2 simulations ($\sim 4.1 \pm 1.0^{\circ}$ C) [Masson-Delmotte et al., 2006]. The discrepancy partly can be explained by additional cooling through changes in atmospheric dust content and vegetation cover, which are not accounted for in PMIP-2 experiments. The magnitude of the extra cooling can be derived from Figure 1, which shows the cooling contribution of the individual forcings. The largest contribution comes from the combined effect of CO₂ (dT_{CO2}, red dots) and ice sheet forcing (dT_{ICE}, light blue dots), which together account for about 75% of total LGM cooling (this includes the effects of a lower sea level and ice sheet elevation on temperature).

[14] The solid red line is calculated by assuming that the temperature response $dT_{\rm CO2}$ is directly proportional to the

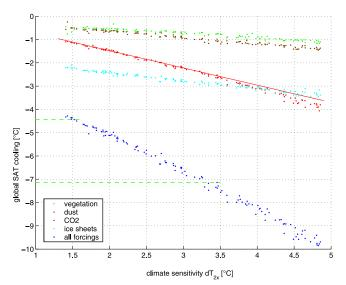


Figure 1. Contribution of individual forcings to global LGM cooling. Shown is the magnitude of simulated global annual SAT cooling between the pre-industrial and LGM climate, arising from the prescription of main glacial forcings. The solid red line represents a theoretical approximation, which assumes a linear relation between the temperature anomaly resulting from lowered CO_2 levels and CO_2 radiative forcing (see main text). Horizontal green lines indicate the cooling range, which is consistent with a tropical Atlantic SST cooling of $3.0 \pm 0.9^{\circ}C$. The climate sensitivity dT_{2x} has been inferred from $2xCO_2$ simulations. See section 2 for the description of calculating individual temperature anomalies.

radiative forcing RF ($dT_{CO2} = \lambda * RF_{CO2}$, with λ being the so-called climate sensitivity parameter). We thus simply have scaled dT by the ratio of glacial to 2xCO₂ forcing. Model versions with high dT_{2x} show slightly larger cooling than estimated from this linear approximation, which assumes the same strength of climate feedbacks for the glacial and modern climate. To test for the dependency of λ on the background climate we have calculated λ for modern (glacial) climate by increasing CO₂ from 280 to 560 ppm (170 to 230 ppm.). The magnitude of λ_{LGM} is comparable to λ_{MOD} for model versions with a climate sensitivity in the lower half of the considered dT_{2x} range. For sensitivities in the upper half systematic differences arise, indicating that the feedback strength is slightly larger for the glacial climate. Thus the difference between approximated and simulated glacial CO₂ cooling can be explained by the difference in the climate sensitivity parameter λ for modern and glacial climate and might be physically interpreted by the larger sea ice and snow albedo feedback acting in a colder climate.

[15] As Figure 1 illustrates, not accounting for the impact of glacial atmospheric dust content and vegetation cover yields for our simulations an underestimation of global LGM cooling by about 1.5°C for a midrange climate sensitivity of 3°C. Orbital changes, despite being the primary cause of the ice ages, do not significantly contribute to global cooling at the LGM and are not separately shown.

4.2. Spatial Characteristics of LGM Cooling

[16] The individual glacial forcings are of different nature, and differ not only in magnitude but as well in their spatial distribution. Figure 2a illustrates the spatial characteristic of the simulated temperature response, resulting

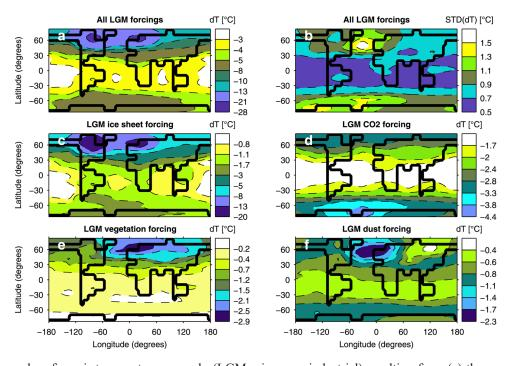


Figure 2. Annual surface air temperature anomaly (LGM minus pre-industrial) resulting from (a) the prescription of all main forcings; (b) the spread from the mean; and annual surface air temperature anomaly (LGM minus pre-industrial) resulting from (c) individual forcings of ice sheets, (d) CO₂, (e) vegetation and (f) dust. All data represent the mean values for the ensemble constrained by tropical SST proxy data.

from the prescription of all glacial forcings. The total LGM cooling is by far strongest over the northern hemisphere ice sheets with maximum cooling about 28°C, moderate tropical cooling (with about 1.6 times larger cooling over land areas than over the oceans) and pronounced Antarctic cooling. The spatial inhomogeneity clearly reveals the imprint of the applied boundary conditions, which is shown in Figures 2c-2f for each individual forcing. Similar to the impact of glacial ice sheets (Figure 2c), vegetation change exerts a pronounced cooling of high northern latitudes (although of much smaller amplitude, Figure 2e). This can be understood by the strong albedo change in northern boreal latitudes through the conversion of forest into tundra. The CO₂ forcing shows a rather uniform temperature response with a characteristic amplification of the cooling toward the poles (Figure 2d). The spatial pattern of glacial radiative dust forcing shows strong inhomogeneities with regions of positive and negative contributions. The prescribed global dust forcing (about -1.2 W/m^2) results in a net cooling, with largest anomalies in the northern Atlantic sector (Figure 2f) through the combined effect of strong negative forcing and sea-ice albedo feedback, which is tightly coupled to the location of North-Atlantic convection sites.

[17] Figure 2b illustrates the standard deviation of all ensemble members shown in Figure 2a. A maximum spread of SAT anomaly is seen in Antarctica and in the North Atlantic, which can be interpreted by the difference in the extent of sea ice area and its impact on the temperature signal through the sea-ice albedo feedback.

4.3. Consistency With Other Regions

[18] Our inferred dT_{LGM} range depends on the accuracy of our applied tropical SST data constraint, which is based on reconstructions from low latitude foraminifera (tropical Atlantic, 20°N-20°S). Recent studies have shown that reconstructed tropical SSTs from geochemical methods agree with estimates derived from faunal transfer functions [Rosell-Melé et al., 2004; Barker et al., 2005]. Systematic differences arise especially in upwelling regions, where geochemical methods suggest a less pronounced maximum cooling. However, as we use cooling averaged over a large area, those differences are not crucial for our analysis. A recent meta-analysis of a broad set of different proxies has inferred mean global tropical cooling [Ballantyne et al., 2005]. If we enlarge our region for comparing model output with proxy data to the whole tropics (30°N-30°S) and use the cooling estimate of this study $(2.7 \pm 1^{\circ}C, 2\sigma)$ we constrain dT_{LGM} very consistently (5.9 \pm 1.7°C).

[19] Would our estimate of global LGM cooling have to be revised if we used proxy information from different regions (besides tropical SSTs) to constrain dT_{LGM} ? Assuming a tropical (30°S–30°N) land cooling of 4–6°C [Farrera et al., 1999], we infer a range of slightly larger dT_{LGM} (6.5 ± 1.1°C). Ice-core data from Antarctica (about 8 ± 2°C surface cooling [Vimeux et al., 2002; Jouzel et al., 2003]) constrain dT_{LGM} very consistently with our tropical SST based estimate to a range of 5.9 ± 1.3°C.

5. Discussion

[20] Although the main glacial forcings are relatively well known, uncertainty in its global magnitude and spatial

pattern remains, especially for dust forcing. The full set of implemented glacial boundary conditions yields a range of 8.0–8.5 Wm⁻² for global mean forcing in our ensemble, with dust and vegetation contributing about 2 Wm⁻² to this estimate. If we repeated our analysis assuming for example, a slightly increased ice sheet forcing, we would constrain the same range of dT_{LGM}, but from a set of model versions with lower climate sensitivities, as long as the latitudinal profile of the glacial temperature anomaly remains unchanged. Yet if, for example, this stronger high latitude forcing only marginally affects the tropical SST decrease (our focus area to constrain the ensemble) but strongly increases high latitude cooling, we then would infer a larger estimate of dT_{LGM}. To check for this uncertainty we replaced the ICE-5G by the ICE-4G ice sheet reconstruction [Peltier, 2004], which yields a somewhat larger ice sheet forcing (globally about 0.5 Wm⁻²). Applying again the tropical SST constraint our new constrained ensemble covers model versions of lower climate sensitivity, but the inferred dT_{LGM} is almost identical for both experiments. (Thus the impact of uncertainty in the glacial forcings is of crucial importance, when the range of likely climate sensitivities is to be estimated, but may not strongly affect our estimate of global LGM cooling (see Schneider von Deimling et al. [2006] for details about LGM constrained climate sensitivity estimates).

[21] A further issue is our simulated relationship between regional LGM cooling and $dT_{\rm LGM}$. Considering that we infer a larger spread between those two characteristics from a multi-model ensemble, we accordingly underestimate the uncertainty of likely LGM cooling by our approach. As presently fully-coupled multi-model ensembles of the LGM climate are not available it is difficult to quantify this effect. We therefore refer to the LGM ensemble study of Annan et al. [2005], who use an atmospheric GCM coupled to a slab ocean with fixed ocean heat transport, and assume a spread five times larger than seen in our ensemble. With this extreme assumption we then have to add an additional uncertainty of about $\pm 0.5^{\circ} \rm C$ to our estimate of global LGM cooling.

[22] Given the consistency of all median values of our considered dT_{LGM} intervals, our results suggest a best guess for global LGM cooling of about 6°C, with about 1.5°C of the temperature anomaly resulting from cooling contributions of glacial atmospheric dust content and vegetation cover.

[23] **Acknowledgments.** The authors are grateful to M. Werner and I. Tegen for providing and discussing the LGM radiative anomaly dust fields, to C. Schäfer-Neth and A. Paul for providing the SST paleo data, to V. Petoukhov and R. Calov for assistance with the simulation design, to M. Flechsig, W. v. Bloh, A. Glauer and K. Kramer for providing the ensemble simulation framework. This work was supported by BMBF research grant 01LG0002, and grant II/78470 by the Volkswagen Foundation.

References

Annan, J., J. Hargreaves, R. Ohgaito, A. Abe-Ouchi, and S. Emori (2005), Efficiently constraining climate sensitivity with ensembles of paleoclimate simulations, Sci. Online Lett. Atmos., 1, 181–184.

Ballantyne, A. P., M. Lavine, T. J. Crowley, J. Liu, and P. B. Baker (2005), Meta-analysis of tropical surface temperatures during the Last Glacial Maximum, Geophys. Res. Lett., 32, L05712, doi:10.1029/ 2004GL021217.

Barker, S., I. Cacho, H. Benway, and K. Tachikawa (2005), Planktonic foraminiferal Mg/Ca as a proxy for past oceanic temperatures: A methodological overview and data compilation for the Last Glacial Maximum, *Quat. Sci. Rev.*, 24(7–9), 821–834.

- Claquin, T., et al. (2003), Radiative forcing of climate by ice-age atmospheric dust, *Clim. Dyn.*, 20, 193–202.
- Farrera, I., et al. (1999), Tropical climates at the Last Glacial Maximum: A new synthesis of terrestrial palaeoclimate data: I. Vegetation, lake levels and geochemistry, Clim. Dyn., 15, 823–856.
- Ganopolski, A. (2003), Glacial integrative modeling, *Philos. Trans. R. Soc. London, Ser. A*, 361(1810), 1871–1883.
- Ganopolski, A., S. Rahmstorf, V. Petoukhov, and M. Claussen (1998), Simulation of modern and glacial climates with a coupled global model of intermediate complexity, *Nature*, 391, 351–356.
- Harrison, S. P., K. E. Kohfeld, C. Roelandt, and T. Claquin (2001), The role of dust in climate changes today, at the Last Glacial Maximum and in the future, *Earth Sci. Rev.*, 54(1–3), 43–80.
- Intergovernmental Panel on Climate Change (2001), Climate Change 2001: The Scientific Basis, edited by J. T. Houghton et al., Cambridge Univ. Press, New York.
- Lorius, C., J. Jouzel, D. Raynaud, J. Hansen, and H. Le Treut (1990), The ice-core record: Climate sensitivity and future greenhouse warming, *Nature*, 347, 139–145.
- Jouzel, J., F. Vimeux, N. Caillon, G. Delaygue, G. Hoffmann, V. Masson-Delmotte, and F. Parrenin (2003), Magnitude of isotope/temperature scaling for interpretation of central Antarctic ice cores, *J. Geophys. Res.*, 108(D12), 4361, doi:10.1029/2002JD002677.
- Masson-Delmotte, V., et al. (2006), Past and future polar amplification of climate change: Climate model intercomparisons and ice-core constraints, *Clim. Dyn.*, 26, 513–529, doi:10.1007/s00382-005-0081-9.
- Peltier, W. R. (2004), Global glacial isostasy and the surface of the ice-age Earth: The ICE-5G (VM2) model and GRACE, *Annu. Rev. Earth Planet. Sci.*, 32, 111–149.

- Petoukhov, V., A. Ganopolski, V. Brovkin, M. Claussen, A. Eliseev, C. Kubatzki, and S. Rahmstorf (2000), CLIMBER-2: A climate system model of intermediate complexity. part I: Model description and performance for present climate, *Clim. Dyn.*, 16, 1–17.
- Rosell-Melé, A., E. Bard, K. Emeis, B. Grieger, C. Hewitt, P. J. Müller, and R. R. Schneider (2004), Sea surface temperature anomalies in the oceans at the LGM estimated from the alkenone- $U_{37}^{K'}$ index: comparison with GCMs, *Geophys. Res. Lett.*, *31*, L03208, doi:10.1029/2003GL018151.
- Sarnthein, M., R. Gersonde, S. Niebler, U. Pflaumann, R. Spielhagen, J. Thiede, G. Wefer, and M. Weinelt (2003), Overview of Glacial Atlantic Ocean Mapping (GLAMAP 2000), *Paleoceanography*, 18(2), 1030, doi:10.1029/2002PA000769.
- Schäfer-Neth, C., and A. Paul (2003), Gridded global LGM SST and salinity reconstruction, ftp.ncdc.noaa.gov/pub/data/paleo/contributions_by_author/paul2003, World Data Cent. for Paleoclimatol., Boulder, Colo.
- Schneider von Deimling, T., H. Held, A. Ganopolski, and S. Rahmstorf (2006), Climate sensitivity estimated from ensemble simulations of glacial climate, *Clim. Dyn.*, *27*, 149–163, doi:10.1007/s00382-006-0126-8.
- Stier, P., J. Feichter, S. Kinne, S. Kloster, E. Vignati, and J. Wilson (2004), The aerosol-climate model ECHAM5-HAM, Atmos. Chem. Phys. Discuss., 4, 5551–5623.
- Vimeux, F., K. M. Cuffey, and J. Jouzel (2002), New insights into Southern Hemisphere temperature changes from Vostok ice cores using deuterium excess correction, *Earth Planet. Sci. Lett.*, 203(3–4), 829–843.

A. Ganopolski, H. Held, S. Rahmstorf, and T. Schneider von Deimling, Potsdam Institute for Climate Impact Research, PO Box 60 12 03, D-14412 Potsdam, Germany. (schneider@pik-potsdam.de)